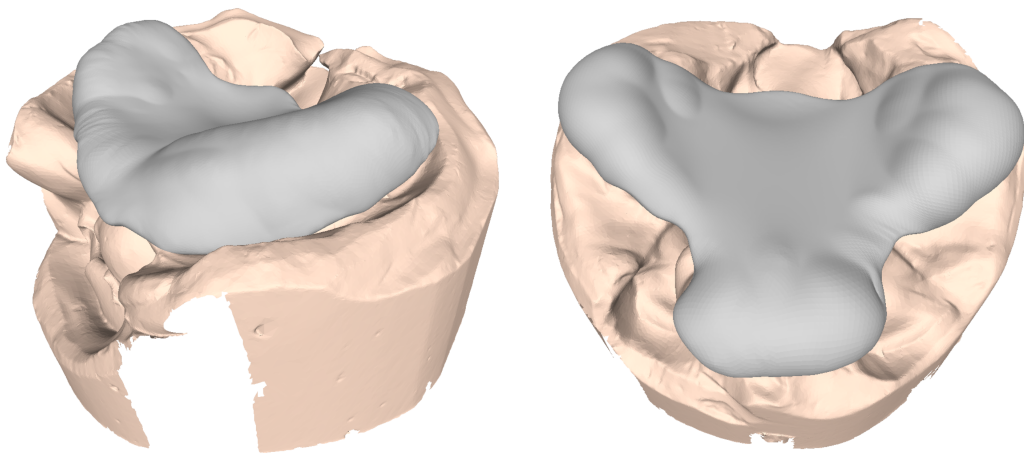


Generalised Automated Plate Computation for Cleft Lip and Palate



Ruben Schenk

Semester Thesis
January 2025

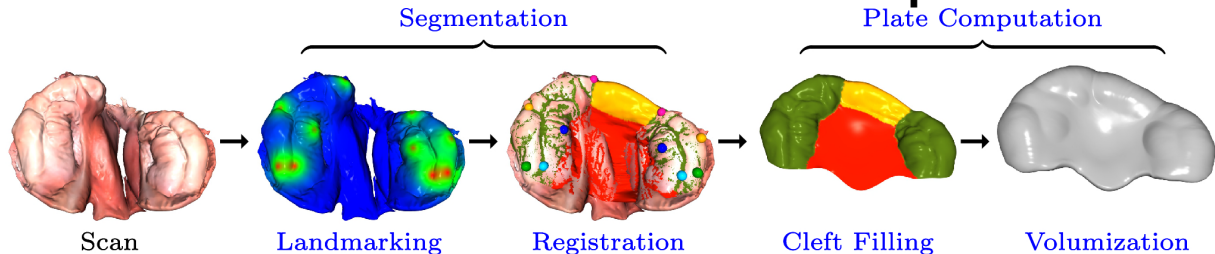
Till Schnabel, Prof. Dr. Barbara Solenthaler

Abstract

Cleft lip and palate are common congenital craniofacial anomalies that often require presurgical orthopedic treatments to align the alveolar ridges and facilitate surgical interventions. Despite advances in digital workflows such as intraoral scanning and 3D printing, current methods face challenges in addressing anatomical complexities, enabling flexible customisation, and automating processes for diverse clinical scenarios. Existing automated pipelines provide robust solutions, but leave room for improvement in flexibility and handling complex cases.

This thesis enhances an established presurgical orthopedic plate design pipeline by introducing three key advancements: improved registration to mitigate plate shrinkage, customisable extensions for better anatomical coverage, and the inclusion of the premaxilla for bilateral cases. These contributions are implemented using enhancements to the Non-Rigid Iterative Closest Point algorithm, As-Rigid-As-Possible deformation techniques, and template modifications.

Together, these advancements improve the robustness, flexibility, and anatomical inclusiveness of the automated pipeline, marking a step towards more efficient and scalable presurgical orthopedic workflows. Although limitations remain, such as improving extension algorithms and refining premaxilla inclusion methods, this work establishes a foundation for future research and development, contributing to the evolving field of digital healthcare solutions for treating cleft lip and palate.

Semester Thesis**Generalized Automated Plate Computation****Introduction**

In collaboration with the University Hospital Basel and the University of Basel, we have developed a fully automated pipeline to compute the 3D geometry of a plate that fits into the mouth of a newborn with cleft lip and palate. As depicted in the figure above, the pipeline accepts the raw intraoral scan as input, predicts landmarks based on a neural network, then registers a common template to the scan, initially driven by the landmarks, then a fixed set of mesh operations, including cutting and Laplacian smoothing, are applied to transform the registered intraoral scan to a fitting plate. The pipeline has been implemented in clinical routine for patients with unilateral cleft lip and palate. However, the pipeline still requires generalization to all cleft types, which requires a more flexible landmarking and registration scheme. Additionally, a nasal stent is currently still added manually to the 3D-printed plate. These shortcomings will be addressed in this semester thesis.

Task Description

The first goal of this thesis is to adjust the registration of bilateral cleft lip and palate cases to ensure the automatically computed plate can be used (close to) 100% of the time in clinical practice. The second goal is to include all remaining cleft types into the pipeline; this includes at least isolated cleft palate and Pierre Robin cases. The student will experiment with a generalized neural network that can predict landmarks (or segment regions) on intraoral scans of all cleft types. Currently, the network is trained per cleft type, which may not be feasible for the remaining cleft types, since they are rarer, thus we have fewer scans of them. The successful completion of these two goals should result in a generalized cleft pipeline that the doctors can use for all children. Frequent feedback from the doctors is essential to achieve this. In case there is time left, the student will explore possibilities to automate the addition of the nasal stent. Since the stent is currently fused via a very thin wire, this may not be appropriate for 3D printing, thus making this bonus goal more challenging.

Skills

- Surface Registration
- Geometry Processing
- Deep Learning

Remarks

A written report and an oral presentation conclude the thesis. The thesis is will be overseen by Prof Barbara Solenthaler and supervised by Till Schnabel.

Contact

For further information, please contact the thesis coordinator (cgl-thesis@inf.ethz.ch)

Contents

List of Figures	vii
1 Introduction	1
2 Background & Related Work	3
2.1 Cleft Lip and Palate Classification	3
2.2 Presurgical Orthopedic Treatment	3
2.2.1 Manual Workflows for Plate Design	5
2.2.2 Digital Workflows for Plate Design	5
2.2.3 Automated Digital Workflows	6
2.3 Non-Rigid Iterative Closest Point Algorithm	7
2.4 As-Rigid-As-Possible Deformation	8
2.5 Summary and Relevance to This Work	9
3 Central Work	11
3.1 Improved Registration with NICP	11
3.1.1 Overview	12
3.1.2 Implementation Details	12
3.1.3 Challenges	13
3.2 Buccal Area Extension via Template Deformation	13
3.2.1 Overview	14
3.2.2 Implementation Details	15
3.3 Premaxilla Inclusion in BCLP Cases	16
3.3.1 Overview	16
3.3.2 Implementation Details	17
3.3.3 Challenges	18

Contents

4	Results	19
4.1	Improved Registration with NICP	19
4.2	Buccal Area Extension via Template Deformation	19
4.3	Premaxilla Inclusion in BCLP Cases	21
5	Conclusion and Outlook	25
5.1	Summary of Contributions	25
5.2	Limitations and Future Work	26
	Bibliography	27

List of Figures

2.1	UCLP deformity	4
2.2	BCLP deformity	4
2.3	Automated pipeline by Schnabel et al.	6
3.1	Illustration of NICP correspondences and filtering condition	13
3.2	Handle and stiff vertex selection in UCLP case	14
3.3	UCLP template extension	16
3.4	Premaxilla inclusion in BCLP cases	17
3.5	BCLP template adaptations	18
4.1	Results of the adapted NICP condition for limited buccal data	20
4.2	Results of the adapted NICP condition for complete buccal data	20
4.3	Buccal area extensions with varying displacements	21
4.4	PM inclusion in BCLP cases	23
4.5	Limitations of PM inclusion in BCLP cases	24

1

Introduction

The integration of advanced technologies into healthcare has revolutionised patient treatment across various domains. From diagnostic imaging to personalised surgical planning, digital workflows and automation are increasingly enabling clinicians to deliver precise and efficient care. In the field of craniofacial anomalies, particularly cleft lip and palate (CLP), these advancements have the potential to significantly enhance treatment outcomes while reducing the burden on both medical professionals and families.

CLP is among the most prevalent congenital craniofacial malformations. According to a recent meta-analysis of 59 studies with 21'088'517 individuals, the prevalence of cleft palate alone is approximately 0.33 per 1000 live births (95% CI: 0.28–0.38), cleft lip alone occurs in 0.30 per 1000 live births (95% CI: 0.26–0.34), and CLP is observed in 0.45 per 1000 live births (95% CI: 0.38–0.52) [SDH⁺22].

Treatment typically involves multiple surgical interventions, starting in infancy and extending into adolescence. Presurgical orthopedic (PSO) treatments, which include the use of custom plates, aim to align alveolar ridges and reduce cleft size, facilitating surgical procedures and reducing the overall surgical burden. PSO treatment has additional benefits such as improved feeding, phonological development, and nasal aesthetics [ABCM17, MSZ⁺10].

Traditional PSO workflows rely on manual techniques, including physical impressions and the creation of plaster models. These approaches are labour-intensive, require specialised skills, and pose risks, particularly to the infant's airway during the impression-taking procedure [Cha95]. Recent advances in digital technologies, such as intraoral scanning and 3D printing, have transformed this workflow into a more efficient and safer process. These technologies allow clinicians to create digital models of the palate, which are then used to design plates via computer-aided design software [KRM⁺18]. However, these methods often demand significant expertise and time, limiting their accessibility and scalability, especially in low-resource settings.

To address these limitations, research has focused on automating the design of presurgical

1 Introduction

plates. Early efforts, such as the RapidNAM framework, introduced semi-automated workflows for designing nasoalveolar moulding devices. Despite demonstrating promising results, these workflows often required manual adjustments, particularly in challenging cases, highlighting the need for fully automated solutions [GRB⁺18, SBGL20, BSG⁺17].

Fully automated digital workflows represent a significant step forward. Schnabel et al. [SGG⁺23] introduced a novel pipeline for generating passive plates for unilateral and bilateral cleft lip and palate. While it has achieved significant success in clinical settings, certain limitations remain. Specifically, the pipeline struggled with plate shrinkage around the alveolar ridge, lacked flexibility for customising plate extensions, and did not adequately support premaxilla coverage in bilateral cleft lip and palate cases.

This thesis aims to address these challenges through three key contributions:

1. Enhancing the Non-Rigid Iterative Closest Point algorithm by introducing constraints to reduce plate shrinkage around the alveolar ridge.
2. Developing a deformation method to extend plates around the ridge by a customisable margin, with integration into the pipeline and GUI for improved usability.
3. Modifying the pipeline to include premaxilla coverage in bilateral cleft lip and palate cases, addressing a clinical desire.

The remainder of this thesis is structured as follows: Chapter 2 reviews related work, detailing advancements in cleft treatment and plate design. Chapter 3 describes the technical methods and improvements introduced in this thesis. Chapter 4 presents the qualitative evaluation of the enhanced pipeline. Finally, Chapter 5 concludes the thesis with a discussion of its contributions, limitations, and potential directions for future work.

2

Background & Related Work

2.1 Cleft Lip and Palate Classification

Cleft deformities are categorised based on the anatomical structures involved. A cleft lip refers to a separation in the upper lip, which may extend to the nose, while a cleft palate involves an opening in the roof of the mouth, affecting the hard and/or soft palate [MM12]. These deformities can occur independently or together, leading to cleft lip and palate (CLP). Each type presents unique anatomical and therapeutic challenges.

Furthermore, clefts are classified as unilateral (UCLP) or bilateral (BCLP) based on the symmetry of the defect. UCLP cases involve a single cleft on one side, as illustrated in Figure 2.1. In contrast, BCLP cases exhibit clefts on both sides of the lip and/or palate, often accompanied by a protruded premaxilla, as depicted in Figure 2.2. The premaxilla's position in BCLP introduces complexities in plate design and surgical planning, necessitating specialised workflows [MM12].

Understanding the classification of cleft types is essential for tailoring automated solutions, as the anatomical differences between UCLP and BCLP significantly influence the registration process, template design, and plate generation workflow. This thesis builds upon these anatomical distinctions to refine and extend the pipeline, ensuring it conforms to the unique challenges presented by each cleft type.

2.2 Presurgical Orthopedic Treatment

In order to narrow the cleft and align the alveolar segments presurgically, patients typically undergo Presurgical Orthopedic (PSO) treatment, where a custom-fitted plate is inserted into the neonate's oral cavity, helping to prevent the tongue from pressing into the cleft. This practice

2 Background & Related Work

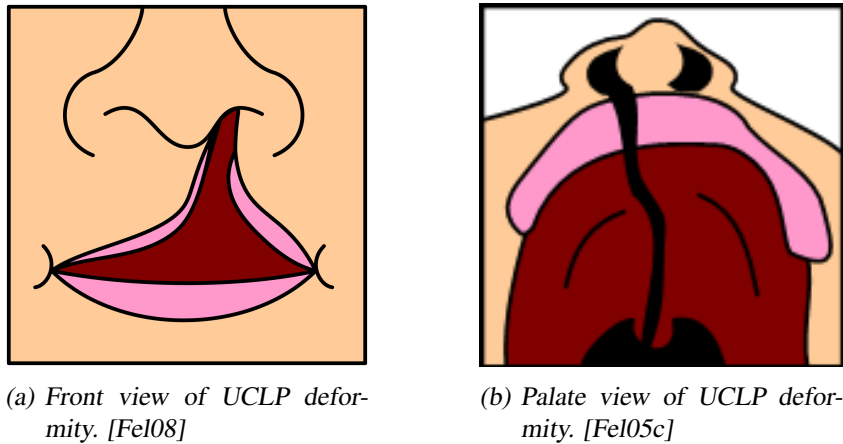


Figure 2.1: Illustrations of UCLP. (a) shows the front view, highlighting the asymmetrical cleft in the lip, while (b) provides the view of the open mouth and palate, indicating the cleft's extent. Images adapted from [Fel08, Fel05c].

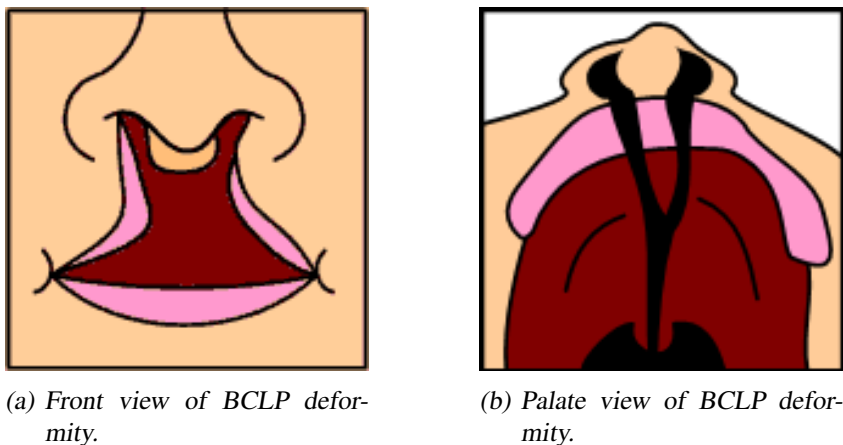


Figure 2.2: Illustrations of BCLP. (a) shows the front view, emphasising the bilateral clefts, while (b) depicts the palate view, revealing the extent of the clefts on both sides. Images adapted from [Fel05a, Fel05b].

can ease subsequent surgical procedures and, in some instances, reduce the number of operations required [MSZ⁺10].

Since its introduction in the 1950s, PSO treatment has seen considerable evolution, spanning a range of passive and active plate designs. Active plates, such as nasoalveolar moulding (NAM) devices [MPS⁺22], apply external forces to simultaneously reshape the alveolar segments, lip, and nasal cartilage. By contrast, passive plates act primarily by bridging the cleft space and preventing excessive tongue pressure on the cleft edges, which can allow gradual narrowing through natural forces in the infant's mouth [ABCM17].

PSO workflows generally involve the following steps:

1. Acquisition of a model of the neonate's oral anatomy, either through physical impressions or digital scanning.

2. Design and fabrication of a plate tailored to the neonate's unique anatomy.
3. Periodic adjustments or replacements of the plate to accommodate growth.

2.2.1 Manual Workflows for Plate Design

Historically, the design of presurgical orthopedic plates has been based on manual, non-digital workflows. A commonly used approach involves taking a physical impression of the neonate's palate. This impression captures the inward contours of the palate and serves as a negative mould. From this mould, a plaster cast is created, which represents the outward geometry of the palate. This cast serves as the foundation for manually sculpting the plate, typically with acrylic materials [ABCM17].

The plate creation process begins with filling the cleft on the plaster cast with modelling material to approximate a healthy palate structure. Monomer sprays and acrylic powders are applied in layers until the plate achieves the desired thickness, which usually ranges between 1.5 mm to 2 mm. While these techniques are effective for crafting custom plates, they are labour-intensive, requiring significant expertise from trained professionals. The reliance on skilled personnel and the inherently subjective nature of the process result in variability in quality, and the approach is not easily scalable. Additionally, taking physical impressions in neonates is associated with risks, such as respiratory obstruction during the procedure, further complicating its widespread adoption [Cha95].

2.2.2 Digital Workflows for Plate Design

Advances in digital technology have significantly streamlined the plate design process by replacing physical impressions and manual sculpting with intraoral scanning and computer-aided design (CAD) tools [KRM⁺18]. These workflows typically involve three key steps:

1. Generating a 3D digital model of the neonate's palate using either an intraoral scanner or by digitising a plaster cast.
2. Designing the plate virtually using CAD software.
3. Fabricating the plate through 3D printing.

For instance, [ZZT⁺22] proposed that once the digital model is acquired, open-source CAD tools, like Meshmixer, enable clinicians to clean the scans, block undercuts, and virtually design plates with precise contours and user-defined parameters. These digital models are subsequently fabricated using biocompatible 3D printing materials, which streamline production and enable rapid iterations. Compared to conventional workflows, digital methods significantly reduce manual labour, improve accuracy, and facilitate direct data storage for clinical and research purposes [ZZT⁺22].

Despite these advancements, challenges remain in the implementation of fully automated solutions, emphasising the need for further research in this field. Fully automated workflows are particularly advantageous as they eliminate the need for specialised expertise, reduce inter-operator variability, and ensure more objective and reproducible results, making them ideal for

widespread clinical adoption. This thesis builds upon these digital advancements by enhancing template registration and deformation methods, enabling robust and customisable plate designs.

2.2.3 Automated Digital Workflows

Early automation efforts, such as RapidNAM [GRB⁺18, SBGL20, BSG⁺17], aim to introduce greater automation by incorporating geometric algorithms for segmenting alveolar ridges and fitting curves to construct the plate. Despite these advancements, workflows like RapidNAM often require manual corrections to resolve segmentation artefacts, which introduces inefficiencies and limits the degree of automation achievable.

Building upon such efforts, Schnabel et al. proposed a fully automated pipeline (Figure 2.3) for the design of passive plates, addressing many of the limitations of earlier approaches [SGG⁺23]. This pipeline provides an end-to-end workflow for both UCLP and BCLP cases, utilising deep learning and advanced geometric processing to automate the entire process, from input scan to a 3D-printable plate.

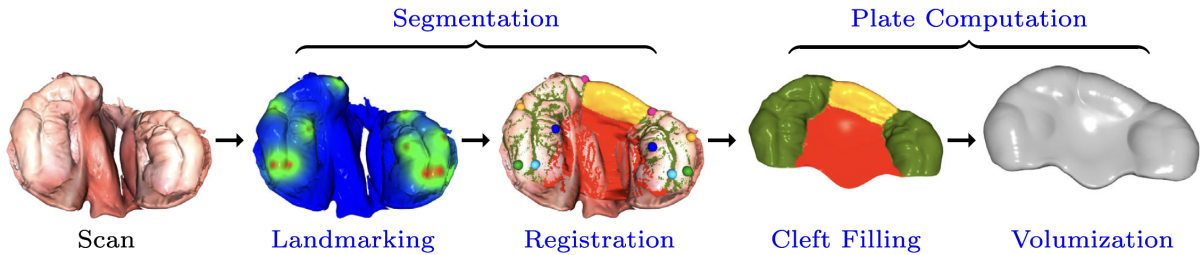


Figure 2.3: The fully automated pipeline proposed by Schnabel et al. [SGG⁺23]. This pipeline combines deep learning for automated landmarking and nonrigid surface registration for automated plate design, from raw intraoral scans to 3D-printable plates. Reproduced with permission from [SGG⁺23].

The pipeline begins with the acquisition of a 3D model of the neonate’s palate, obtained either through intraoral scanning or by digitising a plaster cast. The input scan undergoes automatic landmark detection using DiffusionNet [SACO20], a neural network trained on a dataset of 283 UCLP and 114 BCLP scans. This detection process occurs in two stages: first, coarse landmarks are predicted, and the mesh is aligned to a pre-annotated template using weighted Procrustes analysis. Next, these landmarks are refined for greater precision. Unlike conventional methods, which often use one-hot annotations, Schnabel et al. adopt exponential probability maps, enabling more robust and accurate landmark predictions, even for anatomically complex cases.

Following landmark detection, the pipeline uses the Non-Rigid Iterative Closest Point (NICP) (cf. Chapter 2.3) algorithm to register a template to the patient-specific scan. This algorithm iteratively deforms the template to minimise the distance between the two surfaces while preserving local geometric coherence. The template is pre-segmented into key anatomical regions, such as alveolar ridges and cleft areas, facilitating alignment and ensuring that the registration respects anatomical boundaries.

After successful registration, the plate is generated automatically. The generation involves two key steps: cleft filling and volumisation. In the cleft filling step, the region representing the cleft

is smoothed and filled to approximate a healthy palate. Schnabel et al. employ a sphere-based smoothing approach, ensuring adequate tongue space and avoiding interference with surrounding tissues. The volumisation step then thickens the surface mesh to approximately 2 mm, using curvature-selective smoothing to eliminate self-intersections and ensure smooth transitions, resulting in a clinically viable plate.

This automated workflow achieves significant milestones by reducing the design time to under three minutes while maintaining a high level of accuracy. Clinical validation has demonstrated its effectiveness, with a 100% approval rate for printed plates, subject to minor adjustments, evaluated by cleft care specialists. Compared to earlier frameworks, the pipeline by Schnabel et al. provides a robust and reliable solution for presurgical plate design. However, challenges remain, particularly in addressing complex cases such as BCLP with premaxilla integration and preventing plate shrinkage during registration when parts of the buccal region are missing from the scan data. These limitations highlight opportunities for further development, building on the strong foundation established by this pipeline.

2.3 Non-Rigid Iterative Closest Point Algorithm

The NICP algorithm is a cornerstone of mesh registration, widely used for aligning generic templates to specific meshes. Unlike rigid ICP, which assumes uniform transformations, NICP accommodates large deformations while preserving local geometric structures. The algorithm minimises a composite energy function comprising three distinct terms: the distance term, the stiffness term, and the landmark term, as described in [ARV07].

The first component, the distance term E_d , ensures the template vertices align closely with the target surface by minimising the distance between corresponding points. This term is mathematically defined as:

$$E_d(\mathbf{X}) = \sum_{v_i \in V} w_i \text{dist}^2(T, \mathbf{X}_i v_i),$$

where v_i are the template vertices, T is the closest point on the target surface, \mathbf{X} are the transformation parameters, and w_i are correspondence weights reflecting the reliability of the matches.

The second component, the stiffness term E_s , regularises the deformation by penalising differences between the transformations of neighbouring vertices. This term ensures the smoothness of the deformation field and is expressed as:

$$E_s(\mathbf{X}) = \sum_{\{i,j\} \in E} \|(\mathbf{X}_i - \mathbf{X}_j)\mathbf{G}\|_F^2,$$

where E represents the edges in the mesh graph, \mathbf{G} is a diagonal weighting matrix that incorporates a stiffness parameter, and $\|\cdot\|_F$ denotes the Frobenius norm.

The final component, the landmark term E_l , facilitates alignment by incorporating known correspondences between predefined landmark points. This term is given by:

$$E_l(\mathbf{X}) = \sum_{(v_i, l) \in L} \|\mathbf{X}_i v_i - l\|^2,$$

2 Background & Related Work

where L is the set of known landmark pairs. While this term is optional, it significantly improves registration accuracy in cases where reliable landmarks are available.

The overall cost function of NICP is a weighted sum of these three components:

$$E(\mathbf{X}) = E_d(\mathbf{X}) + \alpha E_s(\mathbf{X}) + \beta E_l(\mathbf{X}),$$

where α and β are regularisation parameters that balance the influence of stiffness and landmarks, respectively. The algorithm iteratively minimises this cost function by alternating between recomputing the correspondences and solving for the deformation parameters \mathbf{X} . At each iteration, the correspondences are redefined, typically resulting in updated, often binary, correspondence weights. Simultaneously, the stiffness weights α and landmark weights β are progressively lowered, gradually drawing the template closer to the target while maintaining stability and ensuring a robust alignment even in cases of complex deformations.

While the NICP algorithm provides a robust framework for template registration, this thesis enhances its capabilities by introducing additional constraints that prevent undesired deformations, such as plate shrinkage.

2.4 As-Rigid-As-Possible Deformation

The As-Rigid-As-Possible (ARAP) deformation algorithm plays a crucial role in applications requiring intuitive and detail-preserving mesh adjustments. By enforcing local rigidity during deformation, ARAP provides a powerful framework for modifying surfaces while maintaining their geometric integrity. The method minimises an energy function that captures the deviation from local rigidity, as introduced in [SA07]:

$$E(\mathcal{S}') = \sum_{i=1}^n w_i \sum_{j \in \mathcal{N}(i)} w_{ij} \|(p'_i - p'_j) - \mathbf{R}_i(p_i - p_j)\|^2.$$

In this formulation, \mathcal{S}' is the deformed mesh, p_i and p_j are the original vertex positions, p'_i and p'_j are their deformed positions, $\mathcal{N}(i)$ represents the set of neighbouring vertices of i , \mathbf{R}_i is the optimal local rotation matrix for vertex i , and w_i, w_{ij} are cell and edge weights, often derived from cotangent weights for mesh regularisation.

The algorithm operates in two primary steps, iteratively solving for the optimal rotations and vertex positions. In the first step, the optimal rotation \mathbf{R}_i is computed for each vertex by minimising local deviations from rigidity. This is achieved using Singular Value Decomposition to ensure the rotations are orthogonal. In the second step, the vertex positions are updated by solving a sparse linear system derived from the energy function. These steps are repeated until the energy stabilises, typically within a few iterations.

The ARAP algorithm forms a critical component of this thesis's contributions, enabling controlled and anatomically faithful template deformations. By leveraging ARAP, this work introduces customisable ridge extensions and ensures smooth transitions between deformed and static regions, improving the overall plate design process.

2.5 Summary and Relevance to This Work

Previous research has established a foundation for PSO plate design, from manual and semi-digital workflows to fully automated pipelines. These works address many clinical challenges but often fall short in handling complex anatomies, achieving robust registration, and enabling flexible customisation. Building on the pipeline by Schnabel et al., this thesis introduces targeted enhancements to the registration process, such as constraints to prevent undesired deformations, and extends deformation capabilities through ARAP-based methods.

3

Central Work

To address specific challenges in plate design, this work introduces three advancements to the automated pipeline established by Schnabel et al [SGG⁺23]. The first improvement focuses on refining the NICP algorithm (cf. Chapter 2.3) by incorporating an additional condition based on the angular alignment between the connecting vector and the surface normal at the target point. This ensures a more robust registration, particularly in areas with incomplete scan data. The second contribution introduces a method for buccal area extension using ARAP deformation (cf. Chapter 2.4), enabling clinicians to adjust the buccal region dynamically to enhance plate stability and fit. Finally, the inclusion of the premaxilla (PM) in the plate design for BCLP cases addresses specific clinical requirements and desires. Each of these contributions builds upon existing methodologies while introducing solutions to improve anatomical accuracy, reduce artefacts, and potentially increase clinical usability.

3.1 Improved Registration with NICP

The original implementation of NICP in the pipeline suffered from plate shrinkage around the buccal area. This issue arose due to faulty registration when aligning the template plate to the patient-specific scan. The algorithm inherently matches each vertex on the template to its nearest point on the target surface. However, in cases where the scans were incomplete or shorter in the buccal area, the closest-point matching process led to invalid correspondences. Specifically, points on the template would match to vertices on the target scan that were directed upwards in direction towards the ridge (cf. Figure 3.1). This resulted in iterative shrinking deformations of the template boundary, causing the plate to shorten undesirably in this region.

3.1.1 Overview

To address this, an additional constraint was introduced in the NICP algorithm to preserve the buccal area's geometry and length. This condition filters matches based on the angular alignment between the connecting vector (from the template vertex to its matched target point) and the normal vector at the target point. By discarding matches that deviate significantly in alignment, the deformation is constrained to preserve the buccal area's geometry. This modification ensures that the registration process avoids undesired shrinking and aligns the template more robustly with the target geometry.

3.1.2 Implementation Details

As seen in Chapter 2.3, one of the energy-terms of the NICP algorithm is the distance term E_d , defined as follows:

$$E_d(\mathbf{X}) = \sum_{v_i \in V} w_i \text{dist}^2(T, \mathbf{X}_i v_i),$$

The key addition lies in modifying the computation of the weights w_i in the above distance term, which determine the influence of each vertex correspondence. Specifically, the added condition ensures that vertices with invalid matches are excluded. For a template vertex \mathbf{v}_i and its corresponding target point \mathbf{u}_i , the weight w_i is adjusted as follows:

1. Compute the connecting vector:

$$\mathbf{c}_i = \mathbf{u}_i - \mathbf{v}_i.$$

2. Normalise the connecting vector:

$$\hat{\mathbf{c}}_i = \frac{\mathbf{c}_i}{\|\mathbf{c}_i\|}.$$

3. Calculate the dot product between the connecting vector and the target normal \mathbf{n}_i :

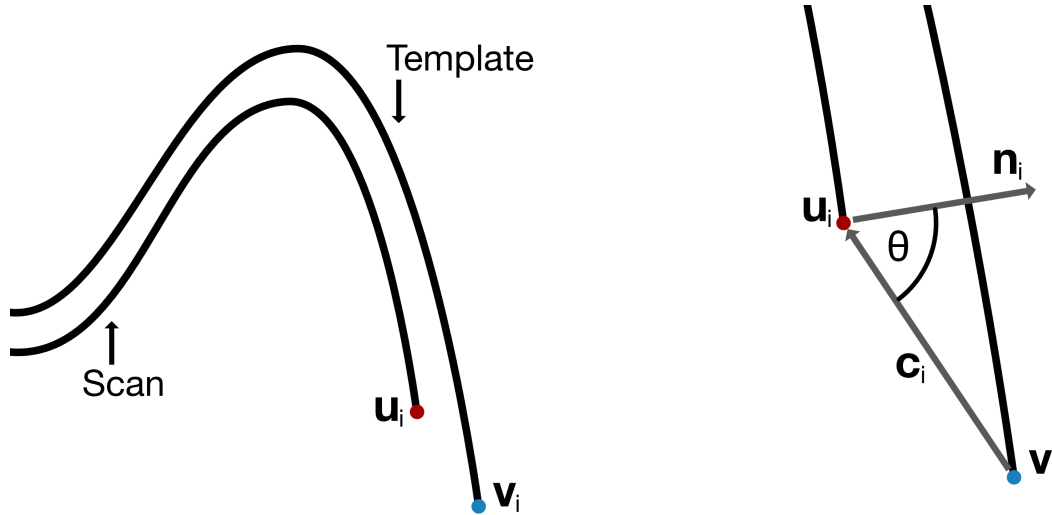
$$\cos \theta = \hat{\mathbf{c}}_i \cdot \mathbf{n}_i.$$

4. Apply the boundary condition to the weight:

$$w_i = \begin{cases} w_i, & \text{if } |\cos \theta| \geq \text{threshold}, \\ 0, & \text{otherwise.} \end{cases}$$

By incorporating this condition, correspondences where the connecting vector deviates significantly from the surface normal (i.e., with θ outside the allowable threshold) are excluded. This prevents template vertices from erroneously shrinking into regions with incomplete or noisy data.

Figure 3.1(a) illustrates the problem of incorrect correspondences in a scan with a shorter buccal area. Figure 3.1(b) zooms in to show the geometric relationship between \mathbf{v}_i , \mathbf{u}_i , the connecting vector \mathbf{c}_i , and the surface normal \mathbf{n}_i .



(a) Illustration showing the ridge and buccal area of a scan and a template. Noticeably, the template has a longer buccal area than the scan.

(b) Detailed view of the condition for invalid matches.

Figure 3.1: Illustration of incorrect correspondences at the buccal region and how the angular constraint improves alignment. (a) Side view of the scan and template, showing that the scan is shorter in the buccal area. (b) Close-up highlighting the geometric relationship between the template vertex v_i , the target point u_i , the connecting vector c_i , and the surface normal n_i . Correspondences with $|\cos \theta|$ below the threshold are excluded.

3.1.3 Challenges

The primary challenge in implementing the boundary condition was selecting an appropriate threshold for $|\cos \theta|$. A small threshold could exclude valid correspondences, especially in areas with high curvature or noise, leading to incomplete registration. Conversely, a large threshold could allow invalid matches, failing to address the original problem of ridge shrinkage.

Extensive experimentation identified 0.95 to be a balanced threshold value that worked robustly across various datasets.

3.2 Buccal Area Extension via Template Deformation

While the NICEP algorithm improvements helped reduced buccal area shrinkage, some clinicians expressed the need for an even more pronounced extension of this region in specific cases. Since the buccal area serves as the primary anchor for the plate in the neonate's mouth, ensuring its proper extension and robustness is crucial for stability and functionality. To accommodate these clinical preferences, an additional pre-registration deformation step was introduced, allowing for customisable buccal area extensions to meet specific requirements.

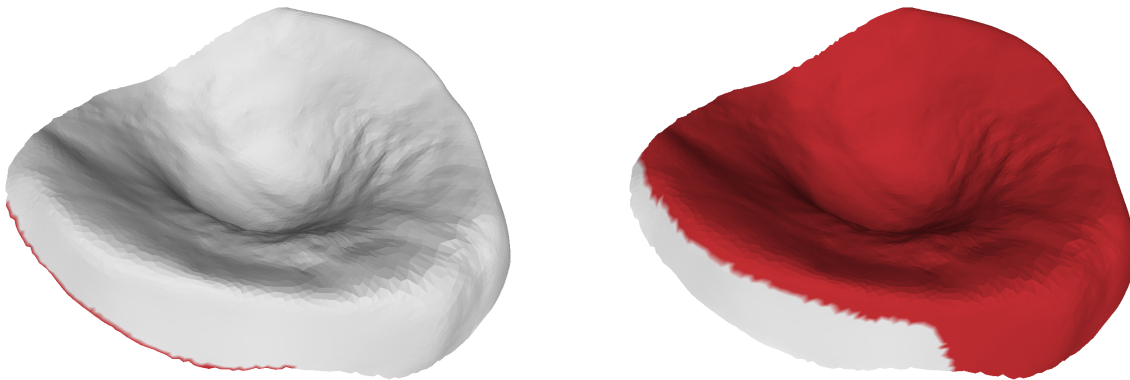
3.2.1 Overview

The buccal area extension process is designed as an optional preprocessing step that dynamically deforms the template to expand its buccal region. The deformation is achieved using the ARAP algorithm, which balances local rigidity with the desired deformation to ensure a natural extension of the buccal area while maintaining the overall integrity of the template.

Two categories of vertices play a key role in the deformation:

- **Handle vertices:** These are boundary vertices along the outer buccal region, selected for displacement (Figure 3.2(a)).
- **Stiff vertices:** These vertices remain fixed to preserve the structure of the template and localise the deformation to the ridge (Figure 3.2(b)).

By displacing the handle vertices outward in a direction dynamically calculated from the local geometry, the buccal area is extended in a manner that respects the natural curvature and orientation of the surrounding structure. This approach ensures that the deformation better aligns with the anatomical features of the buccal area, preserving its shape and continuity as much as possible. A uniform displacement along the $-z$ axis was also tested, but this resulted in unnatural distortions. While the proposed method may not achieve a perfectly smooth deformation, it provides a practical balance between computational simplicity and anatomical fidelity, ensuring a better fit and improved stability of the plate.



(a) Example of handle vertices.

(b) Example of stiff vertices.

Figure 3.2: Visualisation of vertex categories for buccal area extension in the UCLP template. (a) highlights the handle vertices along the buccal boundary, which are displaced during the deformation process, while (b) illustrates the stiff vertices that remain fixed to localise the deformation and maintain template integrity.

3.2.2 Implementation Details

The outward deformation of handle vertices is central to this approach. The deformation direction for each handle vertex is computed dynamically to ensure smooth and anatomically accurate extensions. This involves the following steps:

1. For each handle vertex \mathbf{v}_i , select a neighbourhood of adjacent vertices within the boundary region. The neighbourhood size is defined as a tunable parameter.
2. Compute edge directions between neighbouring vertices:

$$\mathbf{d}_{jk} = \frac{\mathbf{v}_j - \mathbf{v}_k}{\|\mathbf{v}_j - \mathbf{v}_k\|},$$

where \mathbf{v}_j and \mathbf{v}_k are positions of the neighbouring vertices.

3. Average these edge directions to obtain a representative boundary direction:

$$\mathbf{d}_{\text{avg}} = \frac{1}{N} \sum_{j,k} \mathbf{d}_{jk}.$$

4. Compute the outward direction for the vertex using the cross product between the averaged boundary direction and the vertex normal \mathbf{n}_i :

$$\mathbf{d}_{\text{outward}} = \mathbf{n}_i \times \mathbf{d}_{\text{avg}}.$$

5. Ensure that the outward direction aligns approximately with the desired extension axis (typically $-z$). If the alignment is inverted, the outward direction is flipped:

$$\mathbf{d}_{\text{final}} = \begin{cases} \mathbf{d}_{\text{outward}}, & \text{if } \mathbf{d}_{\text{outward}} \cdot \mathbf{z}_{\text{neg}} > 0, \\ -\mathbf{d}_{\text{outward}}, & \text{otherwise.} \end{cases}$$

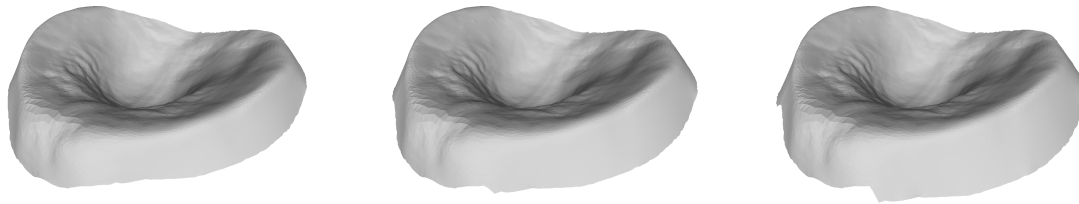
The handle vertices are then displaced along $\mathbf{d}_{\text{final}}$ by a user-defined amount Δd :

$$\mathbf{v}_i^{\text{new}} = \mathbf{v}_i + \Delta d \cdot \mathbf{d}_{\text{final}}.$$

To propagate these displacements smoothly across the entire template, the ARAP deformation method is applied. This ensures that the structural integrity and anatomical relevance of the template are preserved, while accommodating the local extensions.

The template extension is integrated into the pipeline as an optional step, executed before the registration process. The deformation parameters, such as displacement magnitude and neighbourhood size, are configurable to adapt to different clinical requirements.

The extension results, shown in Figure 3.3, demonstrate the effectiveness of the proposed method in generating customisable buccal area expansions while maintaining anatomical relevance.



(a) Original UCLP template. (b) UCLP template, 1 mm extension. (c) UCLP template, 2 mm extension.

Figure 3.3: Comparison of UCLP templates with buccal area extensions. (a) shows the original UCLP template without modifications, while (b) and (c) depict the template after 1 mm and 2 mm buccal area extensions, respectively. All extensions were performed with a neighbourhood size of 9 to calculate the deformation direction.

3.3 Premaxilla Inclusion in BCLP Cases

In the original pipeline, the template for BCLP cases excluded the PM from the plate design. While this approach sufficed in some cases, clinicians expressed a desire for plates that included the PM to stabilise it alongside the alveolar ridges. However, in its initial state, the BCLP template design did not fully bridge the cleft regions, instead following the natural contour of the clefts and running alongside them. While this design was functional for templates excluding the PM, it became problematic when the PM was included in the plate. Specifically, when the plate was cut from the template, the lack of a smooth transition between the ridge and the PM resulted in a plate with noticeable artefacts, such as uneven surfaces, self-intersections, and dips.

3.3.1 Overview

The implementation to include the PM was relatively straightforward and required minimal changes to the pipeline. The process involved two key modifications:

1. **Defining Stiff Regions:** Two stiff regions were defined on the template, corresponding to the expected locations of the clefts (left and right of the PM). These stiff regions ensured minimal deformation in these areas during the registration and smoothing phase of the pipeline (Figure 3.4(a)).
2. **Adapting the Plate Index Set:** The plate index set, which determines the region of the template used for plate generation, was modified to include the PM. This ensured that the PM became an integral part of the final plate design after the registration step (Figure 3.4(b), 3.4(c)).

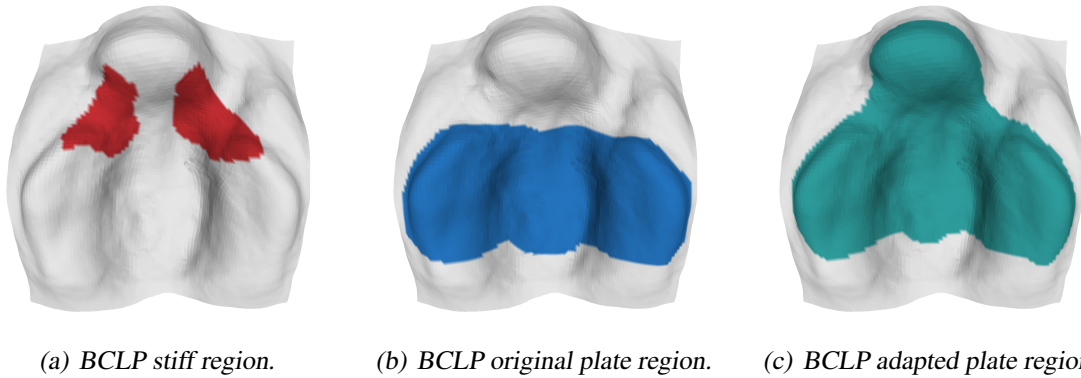


Figure 3.4: Visualisations of template modifications for PM inclusion in BCLP cases. (a) highlights the stiff regions defined in the cleft areas (left and right of the PM) to minimise deformation during registration and smoothing. (b) shows the original plate region that excluded the PM, while (c) depicts the adapted plate region that includes the PM as part of the final design.

3.3.2 Implementation Details

Incorporating the PM into the plate required careful handling of the cleft regions to maintain a smooth transition from the ridge to the PM. Initially, the cleft regions exhibited downward dips that compromised the plate’s smoothness. The implementation to address these issues evolved through two stages.

First Implementation: Initial Inclusion

The first implementation leveraged the existing functionality of the pipeline to define stiff regions and adapt the plate index set. By ensuring minimal deformation in the stiff regions during registration smoothing, the PM was successfully included in the plate. However, this approach led to artefacts where the clefts transitioned into the ridge and PM. Specifically, the plate followed the downward dips in the clefts, resulting in irregularities that hindered its smoothness.

Improved Implementation: Pre-Smoothing the Template

To address these issues, two potential solutions were considered:

- **Line-Based Smoothing:** Define two lines for each cleft – one along the ridge side and one along the PM side – and smooth the region between these lines after registration. This approach would automatically lift the region and reduce artefacts.
- **Template Pre-Smoothing:** Manually adjust the template to smooth the region between the ridge and the PM (where the clefts are) before running the pipeline. This simpler approach required fewer changes to the pipeline and was chosen due to time constraints.

The selected approach involved manually pre-smoothing the cleft regions of the template, creating a more uniform and gradual transition from the ridge to the PM. This adjustment significantly reduced artefacts in the final plate and ensured the stability of the stiff regions during

3 Central Work

registration and smoothing. Additionally, the template was cut to define clear boundaries along the ridge, facilitating effective extension of the buccal area. The different steps of the template modifications are illustrated in Figure 3.5.

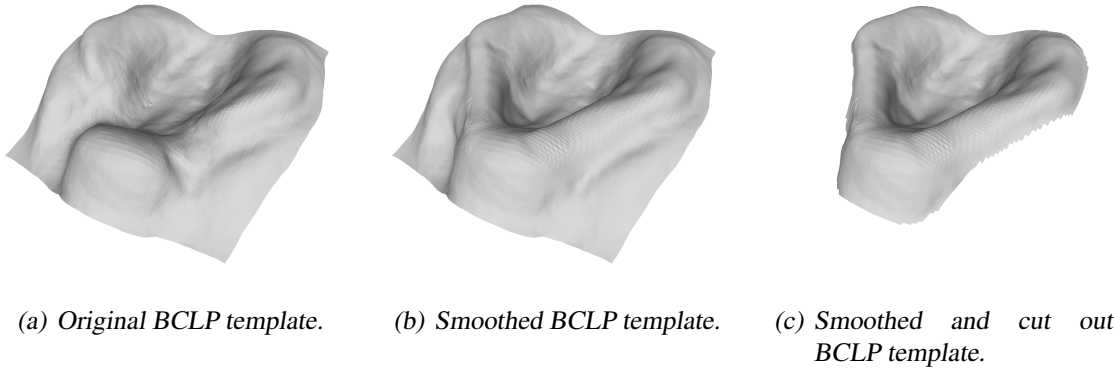


Figure 3.5: Comparison of template modifications for PM inclusion in BCLP cases. (a) shows the original BCLP template, which included excess geometry extending beyond the oral region. (b) illustrates the manually smoothed template, with a more uniform transition between the ridge and PM. (c) depicts the smoothed and cut template, where excess geometry was removed to enable proper boundary definitions along the buccal area, facilitating the extension process.

3.3.3 Challenges

One of the primary challenges was achieving a smooth and artifact-free transition between the ridge and the PM. The chosen pre-smoothing approach, applied once to the template before its integration into the pipeline, proved effective in creating a consistent and functional design for all BCLP cases.

Automated solutions, such as the line-based smoothing approach, could provide a more generalisable alternative by dynamically adapting to individual scans. This flexibility could better accommodate variations in patient anatomy while ensuring smooth transitions and optimal plate design.

4

Results

This chapter presents the results of the implemented modifications to the automated plate pipeline, evaluating their effectiveness in addressing the challenges outlined in Chapter 3. The findings focus on three main areas: (1) the impact of the improved NICP condition, (2) the effect of buccal area extensions, and (3) the inclusion of the PM in plates for BCLP cases. Each section is supported by visual comparisons to illustrate the outcomes.

4.1 Improved Registration with NICP

The adapted NICP condition was evaluated to mitigate plate shrinkage in the buccal area by improving the registration between the template and the scan. Figure 4.1 shows results for a scan where the buccal region contains minimal data. The adapted pipeline generates a plate with a slight extension of approximately 0.5 mm to 1 mm in the buccal area compared to the original pipeline. In Figure 4.2, a scan with more complete buccal data demonstrates even less pronounced extension, as the registration is already closer to the target geometry.

These results confirm the effectiveness of the adapted pipeline in reducing shrinkage and maintaining ridge geometry. However, they also highlight that for cases requiring significant extensions, additional preprocessing, such as the dynamic buccal area extension (cf. Chapter 3.2), is essential.

4.2 Buccal Area Extension via Template Deformation

Buccal area extensions were applied to the template to provide clinicians with the flexibility to extend the area as needed. Figure 4.3 shows the results of 0 mm (no extension), 1 mm, and

4 Results

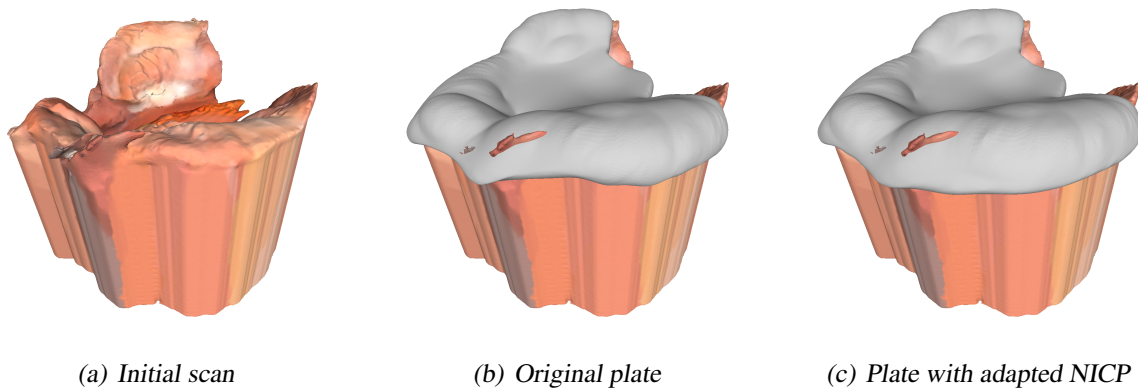


Figure 4.1: Comparison of the original and adapted NICP pipeline for a scan with limited buccal data. (a) shows the initial scan, highlighting the sparse coverage of the buccal region, which is a common limitation of intraoral scans compared to plaster casts. (b) depicts the plate generated by the original pipeline, and (c) illustrates the plate generated by the adapted pipeline, which achieves a slight extension (0.5 mm to 1 mm) in the buccal area.

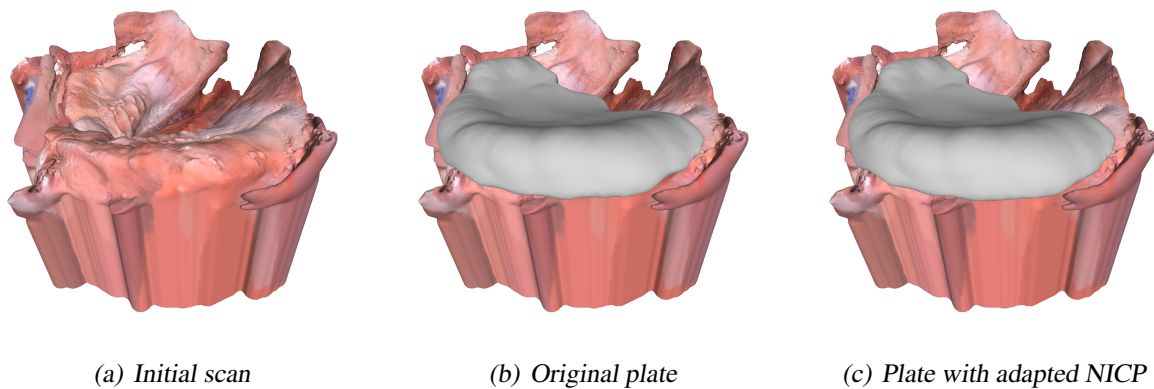


Figure 4.2: Comparison of the original and adapted NICP pipeline for a scan with more complete buccal data. (a) shows the initial scan, (b) depicts the plate generated by the original pipeline, and (c) illustrates the plate generated by the adapted pipeline, where the extension in the buccal area is less pronounced.

2 mm buccal area extensions across three different scans, with each row representing a separate case.

The results demonstrate that the extensions enhance coverage of the buccal area, offering more adaptable templates for varying clinical requirements. The 1 mm extension improves coverage while maintaining alignment with the scan, whereas the 2 mm extension provides further extension but may require careful consideration to avoid potential misalignments with non-relevant regions.

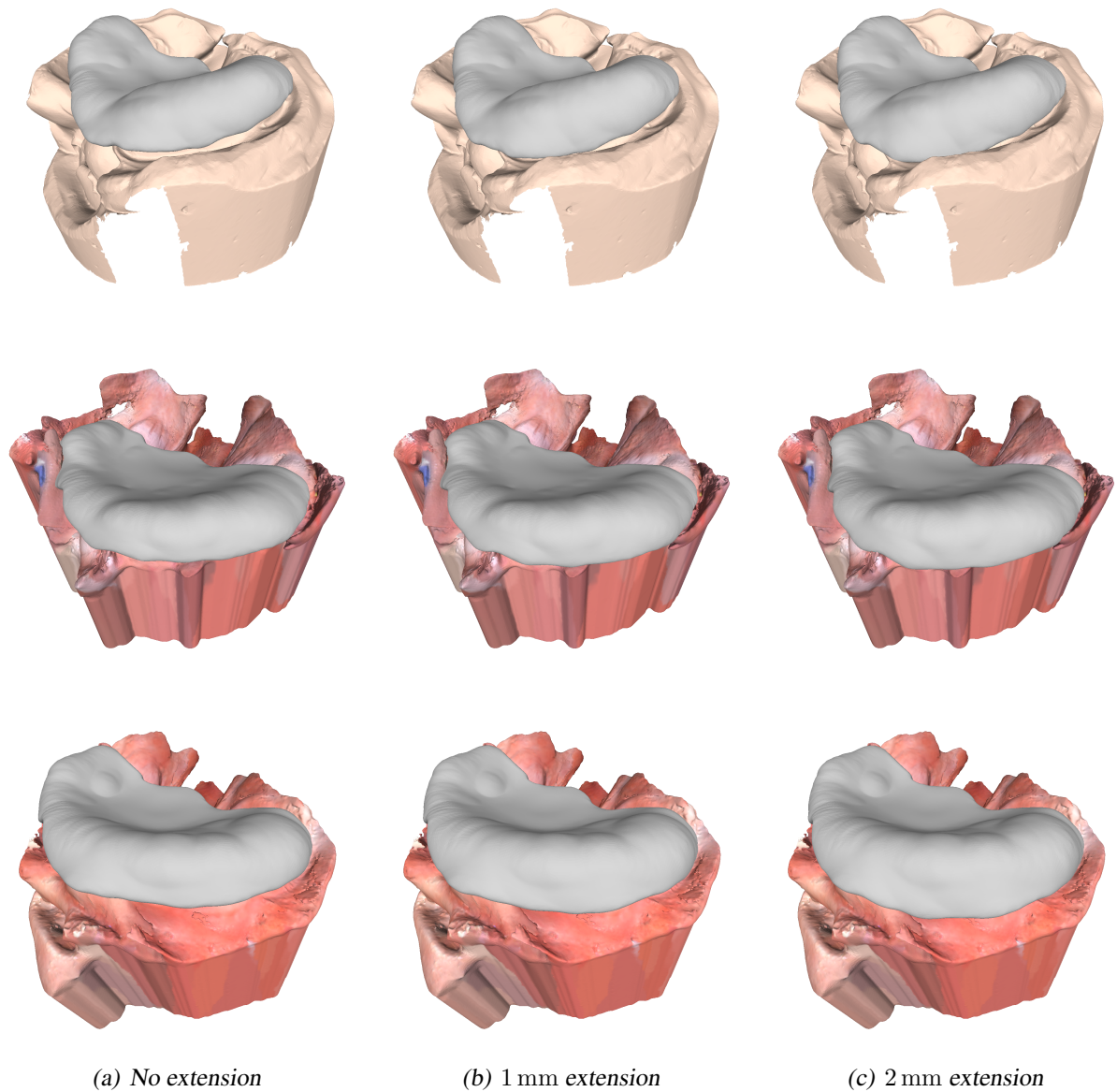


Figure 4.3: Comparison of buccal area extensions across three different scans with 0 mm (no extension), 1 mm, and 2 mm displacements. Each row represents a separate scan, showcasing how the ridge extensions affect the buccal area coverage. The results highlight the versatility of the proposed approach in accommodating different anatomical features.

4.3 Premaxilla Inclusion in BCLP Cases

In BCLP cases, the inclusion of the PM in the plate was achieved by adapting the plate index set and pre-smoothing the template. Figure 4.4 illustrates three cases, showing the original scans alongside the generated plates that include the PM.

The adapted pipeline successfully integrates the PM into the plate, offering a first working solution for BCLP cases. This approach stabilises the PM and connects it to the ridge. While the method generally achieves the desired outcome, some challenges persist, particularly in

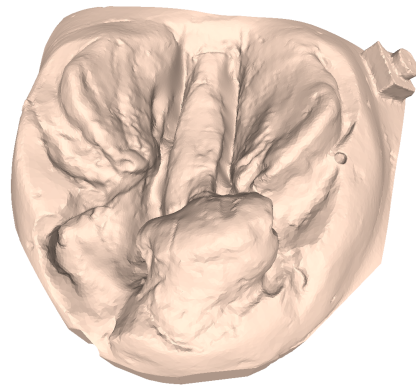
4 Results

ensuring smooth transitions between the PM and the ridge and addressing cases where the PM has more pronounced deformities or misalignment.

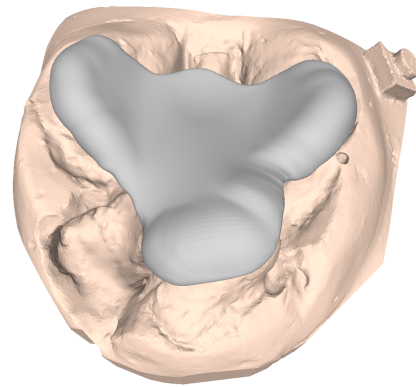
To illustrate these limitations, Figure 4.5 highlights two specific cases. The first row shows incomplete PM coverage, where the plate does not extend fully over the PM. The second row depicts misalignment, where the plate fails to follow the twisted shape of the PM. Both issues suggest that increasing the weight of PM-specific landmarks or adding additional landmarks during registration could improve outcomes.

Overall, while the PM inclusion approach is functional, additional refinements are needed to enhance robustness and handle cases with significant PM deformities. Further research could explore dynamic weighting strategies or localised smoothing to address these challenges.

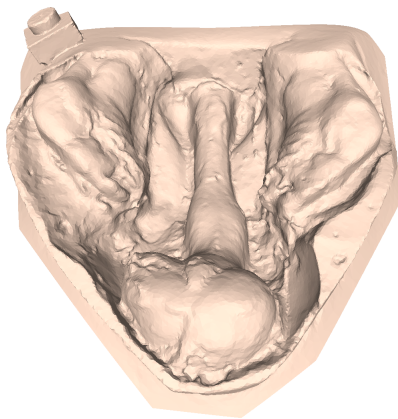
4.3 Premaxilla Inclusion in BCLP Cases



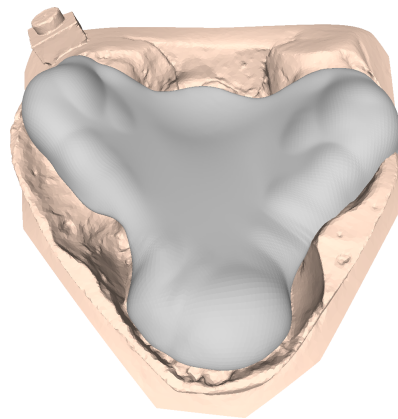
(a) Original scan



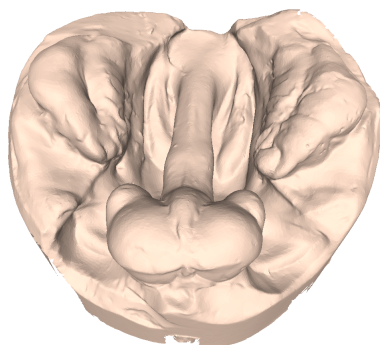
(b) Scan and generated plate, including PM



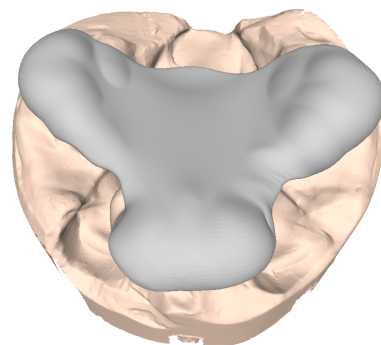
(c) Original scan



(d) Scan and generated plate, including PM



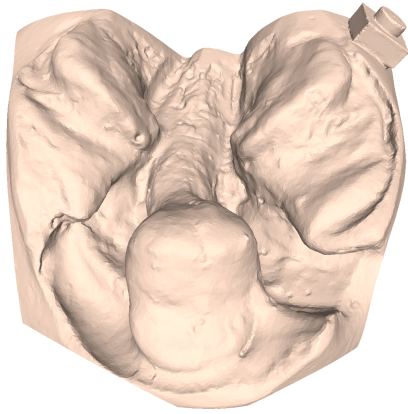
(e) Original scan



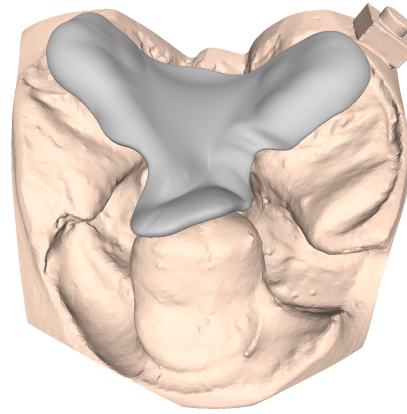
(f) Scan and generated plate, including PM

Figure 4.4: Comparison of original scans (left column) and scans with generated plates including the PM (right column). Each row represents a different case, showcasing how the adapted pipeline incorporates the PM into the plate design. The results demonstrate the feasibility of this approach in providing stability to the PM during PSO treatment.

4 Results



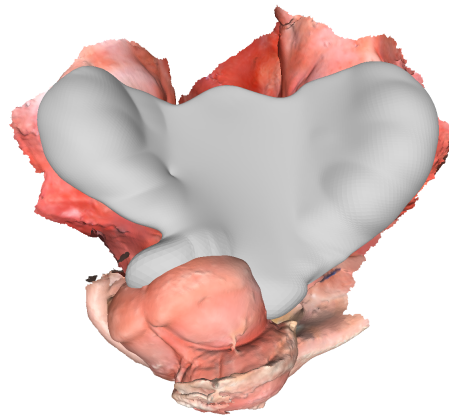
(a) Original scan



(b) Scan and plate, showing incomplete PM coverage



(c) Original scan



(d) Scan and plate, showing misalignment with twisted PM

Figure 4.5: Examples of limitations in the inclusion of the PM. The first row shows a case where the plate does not fully cover the PM. The second row illustrates a case where the plate does not closely follow the alignment of the PM, particularly when the PM is twisted. Addressing these issues may require increasing the weight of PM landmarks or introducing additional PM-specific landmarks.

5

Conclusion and Outlook

This thesis presented three key advancements in the automated pipeline for presurgical orthopedic plate design: improving registration through an adapted NICP condition, introducing buccal area extensions, and incorporating the PM in BCLP cases. These contributions addressed specific challenges related to registration robustness, template adaptability, and anatomical inclusiveness, enhancing the pipeline's capabilities and usability.

5.1 Summary of Contributions

The first contribution focused on refining the NICP algorithm by introducing an angular constraint between the connecting vector and the target surface normal. This modification improved registration quality, particularly by reducing plate shrinkage in the buccal area. The results demonstrated the effectiveness of this approach in mitigating shrinkage; however, in cases with sparse buccal data, the solution remains limited, highlighting the need for additional preprocessing methods.

The second contribution introduced buccal area extensions using ARAP deformation. This method allowed for customisable buccal area extensions, offering clinicians the flexibility to adapt the template to specific patient anatomies. The results showed that the extensions improved buccal coverage, though excessive extensions could lead to misalignments with non-relevant scan regions, such as artefacts or casting blocks. This shows the importance of balancing extension magnitude and scan quality while exploring potential enhancements to the deformation algorithm.

The third contribution addressed the inclusion of the PM in BCLP cases by adapting the plate index set and pre-smoothing the template. This approach successfully integrated the PM into the plate design, stabilising it and connecting it to the ridge. Despite this success, challenges such as ensuring smooth transitions, addressing significant PM deformities, and managing occasional

misalignments remain. These results emphasise the need for further research to refine PM inclusion methods and align plate designs with clinical preferences.

5.2 Limitations and Future Work

While this work demonstrated significant advancements, several limitations highlight areas for improvement.

For the buccal area extensions, the current approach relies on displacing boundary vertices outward in a defined direction. While effective, this method is limited in anatomical accuracy and requires manual adjustment of extension parameters, which can be error-prone. An automated solution to ensure the buccal area is always sufficiently extended would be ideal. Such a solution could involve dynamically analysing the initial scan for areas of sparse data coverage, particularly in the buccal region, and automatically determining optimal extension parameters. This could be achieved by incorporating machine learning models trained to detect under-scanned areas and propose extensions based on typical anatomical features. Alternatively, heuristic approaches leveraging geometric analysis – such as measuring distances between the ridge and boundary regions or assessing curvature consistency – could be implemented to guide automated extensions. These strategies would ensure more consistent outcomes and reduce the need for manual intervention.

Additionally, the pipeline could be enhanced to better support extended templates. Excessive extensions in the current setup occasionally caused the plate to align with fragments or artefacts in the scan, such as casting blocks or noise. Future work could address this by refining the alignment algorithm to prioritise anatomically relevant regions and filter out artefacts during registration.

For PM inclusion, key limitations include achieving smooth transitions between the ridge and PM, addressing cases where the PM is excluded or misaligned, and refining the plate region. Further research should involve feedback from clinicians to better define how the plate should include the PM and ensure it aligns with clinical requirements. Immediate fixes could include implementing localized smoothing methods, refining the plate index set, improving stiff region definitions, and experimenting with additional or weighted PM landmarks to enhance registration accuracy.

Bibliography

- [ABCM17] Ibtesam Alzain, Waeil Batwa, Alex Cash, and Zuhair A Murshid. Presurgical cleft lip and palate orthopedics: an overview. *Clinical, Cosmetic and Investigational Dentistry*, Volume 9:53–59, May 2017.
- [ARV07] Brian Amberg, Sami Romdhani, and Thomas Vetter. Optimal Step Nonrigid ICP Algorithms for Surface Registration. In *2007 IEEE Conference on Computer Vision and Pattern Recognition*, pages 1–8, Minneapolis, MN, USA, June 2007. IEEE.
- [BSG⁺17] Franz Xaver Bauer, Markus Schönberger, Johannes Gattinger, Markus Eblenkamp, Erich Wintermantel, Andrea Rau, Florian Dieter Güll, Klaus-Dietrich Wolff, and Denys J. Loeffelbein. RapidNAM: generative manufacturing approach of nasoalveolar molding devices for presurgical cleft lip and palate treatment. *Biomedical Engineering / Biomedizinische Technik*, 62(4):407–414, August 2017.
- [Cha95] R. A. C. Chate. A Report on the Hazards Encountered When Taking Neonatal Cleft Palate Impressions (1983–1992). *British Journal of Orthodontics*, 22(4):299–307, November 1995.
- [Fel05a] Felsir. Bilateral complete cleft lip. <https://commons.wikimedia.org/wiki/File:CleftLip3.png>, 2005. Accessed: 2025-01-13.
- [Fel05b] Felsir. Bilateral complete cleft lip. <https://commons.wikimedia.org/wiki/File:Cleftpalate2.png>, 2005. Accessed: 2025-01-13.
- [Fel05c] Felsir. Unilateral complete cleft lip. <https://commons.wikimedia.org/wiki/File:Cleftpalate1.png>, 2005. Accessed: 2025-01-13.
- [Fel08] Felsir. Unilateral complete cleft lip. <https://commons.wikimedia.org/wiki/File:Cleftlip2.svg>, 2008. Accessed: 2025-01-13.
- [GRB⁺18] Florian D. Grill, Lucas M. Ritschl, Franz X. Bauer, Andrea Rau, Dominik Gau,

Bibliography

Maximilian Roth, Markus Eblenkamp, Klaus-Dietrich Wolff, and Denys J. Loeffelbein. A semi-automated virtual workflow solution for the design and production of intraoral molding plates using additive manufacturing: the first clinical results of a pilot-study. *Scientific Reports*, 8(1):11845, August 2018.

- [KRM⁺18] Karl-Friedrich Krey, Anja Ratzmann, Philine Henriette Metelmann, Marcel Hartmann, Sebastian Ruge, and Bernd Kordaß. Fully digital workflow for presurgical orthodontic plate in cleft lip and palate patients. *International Journal of Computerized Dentistry*, 21(3):251–259, 2018.
- [MM12] P.A. Mossey and B. Modell. Epidemiology of Oral Clefts 2012: An International Perspective. In M.T. Cobourne, editor, *Frontiers of Oral Biology*, volume 16, pages 1–18. S. Karger AG, 2012.
- [MPS⁺22] Dr. Nikhil Mahajan, Dr. Amrita Puri, Dr. Anshul Singla, Dr. Devansh Kumar, Dr. Shruti Sharma, Dr. Srishti Sureka, and Dr. Mathew Koshy Vaidyan. Nasoalveolar molding: A review. *International Journal of Applied Dental Sciences*, 8(2):451–454, April 2022. Publisher: AkiNik Publications.
- [MSZ⁺10] Brijesh Mishra, Arun K. Singh, Javed Zaidi, G. K. Singh, Rajiv Agrawal, and Vijay Kumar. Presurgical nasoalveolar molding for correction of cleft lip nasal deformity: experience from northern India. *Eplasty*, 10:e55, July 2010.
- [SA07] Olga Sorkine and Marc Alexa. As-Rigid-As-Possible Surface Modeling, 2007. Artwork Size: 8 pages ISBN: 9783905673463 ISSN: 1727-8384 Pages: 8 pages Publication Title: Geometry Processing.
- [SACO20] Nicholas Sharp, Souhaib Attaiki, Keenan Crane, and Maks Ovsjanikov. Diffusion-Net: Discretization Agnostic Learning on Surfaces, 2020. Version Number: 3.
- [SBGL20] Jonas Schiebl, Franz Xaver Bauer, Florian Grill, and Denys J. Loeffelbein. Rapid-NAM: Algorithm for the Semi-Automated Generation of Nasoalveolar Molding Device Designs for the Presurgical Treatment of Bilateral Cleft Lip and Palate. *IEEE Transactions on Biomedical Engineering*, 67(5):1263–1271, May 2020.
- [SDH⁺22] Nader Salari, Niloofar Darvishi, Mohammadbagher Heydari, Shadi Bokae, Fateme Darvishi, and Masoud Mohammadi. Global prevalence of cleft palate, cleft lip and cleft palate and lip: A comprehensive systematic review and meta-analysis. *Journal of Stomatology, Oral and Maxillofacial Surgery*, 123(2):110–120, April 2022. Publisher: Elsevier BV.
- [SGG⁺23] Till N. Schnabel, Baran Gözcü, Paulo Gotardo, Lasse Lingens, Daniel Dorda, Frawa Vetterli, Ashraf Emhemmed, Prasad Nalabothu, Yoriko Lill, Benito K. Benitez, Andreas A. Mueller, Markus Gross, and Barbara Solenthaler. Automated and data-driven plate computation for presurgical cleft lip and palate treatment. *International Journal of Computer Assisted Radiology and Surgery*, 18(6):1119–1125, April 2023.
- [ZZT⁺22] Parichehr Zarean, Paridokht Zarean, Florian M. Thieringer, Andreas A. Mueller, Sabine Kressmann, Martin Erismann, Neha Sharma, and Benito K. Benitez. A Point-of-Care Digital Workflow for 3D Printed Passive Presurgical Orthopedic

Plates in Cleft Care. *Children*, 9(8):1261, August 2022.



Eidgenössische Technische Hochschule Zürich
Swiss Federal Institute of Technology Zurich

Declaration of originality

The signed declaration of originality is a component of every written paper or thesis authored during the course of studies. In consultation with the supervisor, one of the following three options must be selected:

- I confirm that I authored the work in question independently and in my own words, i.e. that no one helped me to author it. Suggestions from the supervisor regarding language and content are excepted. I used no generative artificial intelligence technologies¹.
- I confirm that I authored the work in question independently and in my own words, i.e. that no one helped me to author it. Suggestions from the supervisor regarding language and content are excepted. I used and cited generative artificial intelligence technologies².
- I confirm that I authored the work in question independently and in my own words, i.e. that no one helped me to author it. Suggestions from the supervisor regarding language and content are excepted. I used generative artificial intelligence technologies³. In consultation with the supervisor, I did not cite them.

Title of paper or thesis:

Generalised Automated Plate Computation for Cleft Lip and Palate

Authored by:

If the work was compiled in a group, the names of all authors are required.

Last name(s):

Schenk

First name(s):

Ruben William Gaudenz

With my signature I confirm the following:

- I have adhered to the rules set out in the Citation Guide.
- I have documented all methods, data and processes truthfully and fully.
- I have mentioned all persons who were significant facilitators of the work.

I am aware that the work may be screened electronically for originality.

Place, date

Bern, 19.01.2025

Signature(s)



If the work was compiled in a group, the names of all authors are required. Through their signatures they vouch jointly for the entire content of the written work.

¹ E.g. ChatGPT, DALL E 2, Google Bard

² E.g. ChatGPT, DALL E 2, Google Bard

³ E.g. ChatGPT, DALL E 2, Google Bard